3D Edge Finite Element Solution for Scattered Electric Field using a Direct Solver Parallelized on an SMP Workstation

Michal Kordy[1,2], Virginie Maris[1], Phil Wannamaker [1] and Elena Cherkaev[2]
[1]Energy and Geoscience Institute at the University of Utah
[2]Department of Mathematics at the University of Utah

SUMMARY

We have implemented an edge finite element solution to simulate the Helmholtz equation for scattering of the electric field from subsurface electrical conductivity structure. First-order elements on hexahedral grid are used where the electric field is constant along the edges and varies linearly between edges. Choosing this basis allows the incorporation of topography through deformation of the mesh, and yields a relatively compact system matrix structure. The frequency range considered is appropriate for diffusive EM propagation in a conducting earth, but we retain dielectric properties for the air medium. A secondary E-field formulation is used that facilitates arbitrary impressed sources, which we have tested so far using plane-wave (MT) source fields. Several factors discussed herein have motivated us to migrate from iterative to direct system matrix solvers. Using a matrix tiling approach too parallelizing the modified Cholesky (LDLT) factorization, we have achieved excellent scalability on a 24-core workstation with 0.5 TB RAM. However, use of a direct solution even with double precision arithmetic does not necessarily escape parasitic E-fields in the form of gradient of a scalar potential, especially in the air. Hence, a divergence correction also using a parallelized direct solver was implemented and successfully recovers the correct field. The magnetic field, obtained by curl of E, is not affected by this problem. Good agreement using this solution is obtained for conductive and resistive prisms in a half space, and for a simple hill structure, in comparison to other approaches.

Keywords: forward modeling, finite element, divergence correction, multicore CPU, direct solver, edge elements

FINITE ELEMENT FORMULATION

Consider Maxwell's equations in the frequency domain with $e^{i\omega t}$ time dependence, with the electric source J^{imp}:

$$\begin{cases} \nabla \times E &= -i\omega\mu H \\ \nabla \times H &= \hat{\sigma}E + J^{imp}\,, \qquad \hat{\sigma} = \sigma + i\omega\epsilon \end{cases} \tag{1}$$

The weak form of the equation for E, with homogeneous tangential Dirichlet boundary conditions, is given below:

$$\int_\Omega \frac{1}{\mu}\nabla \times E \cdot \nabla \times K + i\omega \int_\Omega \hat{\sigma}E \cdot K = \int_\Omega J^{imp} \cdot K \tag{2}$$

satisfied for all $K \in H_0(\nabla\times)$. The solution of this equation E is in the same space $H_0(\nabla\times)$, defined as a family of vector fields $K : \Omega \to \mathbb{C}^3$, such that:

$$\int_\Omega ||K||^2 + \int_\Omega ||\nabla \times K||^2 < \infty, \;\; n \times K|_{\partial\Omega} = 0$$

For a finite mesh, $H_0(\nabla\times)$ space is replaced with finite dimensional space $H_0^h(\nabla\times)$ of linear combinations of first order edge shape functions N_i where i is an edge index. A linear system of equations is obtained

$$Ax = b \tag{3}$$

$$A_{i,j} = \left[\int_\Omega \frac{1}{\mu}\nabla \times N_i \cdot \nabla \times N_j + i\omega \int_\Omega \hat{\sigma}N_i \cdot N_j\right] \tag{4}$$

$$b_i = \int_\Omega J^{imp} \cdot N_i \tag{5}$$

Vector x contains coefficients of a linear combination of shape functions. The approximation of the electric field is

$$E = \sum_{i=1}^{n_e} x_i N_i \tag{6}$$

Magnetic field is then calculated from (1) as

$$H = \frac{-\nabla \times E}{i\omega} \tag{7}$$

PARALLEL DIRECT SOLVER

There are several reasons why a direct solver is considered in this paper. Because of the presence of the air in the domain, and as a result the small value of $\omega\hat{\sigma} = \omega^2\epsilon_0$, especially for small frequencies, the system matrix is ill conditioned. The condition number is further increased if element aspect ratios become extreme which is a common issue with a structured hexahedral mesh if the mesh boundaries are to be sufficiently far from the center of the domain. High condition number causes an iterative solution to be slow. Moreover, some geoelectrical methods as well as direct Gauss-Newton inversion approaches require that many source vectors be solved; this can become much more efficient with direct solutions once the system matrix has been factored. Finally, recent advances in the power of symmetric multiprocessing (SMP) computers make available an affordable, single-box workstation with numerous cores to parallelize and up to 1 TB of memory.

The system matrix is symmetric, complex valued and, for a structured grid, banded. As a result LDLT factorization will result in L matrix that has the same bandwidth as the original matrix. This allows one to store only the portion of the matrix within the outer band (2% of the memory is required for the biggest model considered in this paper, with 97x97x50 elements). We discuss parallel factorization at a later point.

DIVERGENCE CORRECTION

Even though a direct solver is used, because of finite precision (double precision is used here), the electric field in the air can experience oscillatory behavior especially toward low frequencies. This is due to a parasitic solution of the form $\nabla\varphi$, which is added to the true solution (e.g., (Smith, 1996)). This error requires a divergence correction to the electric field.

For $H_0(\nabla\times)$ space, there exists a Hodge decomposition (Bochev & Gunzburger, 2006), a decomposition into the range of the gradient $R(\nabla)$ (which is equal to the null space of the curl) and the space orthogonal to it $R(\nabla)^{\perp_{\hat{\sigma}}}$:

$$H_0(\nabla\times) = R(\nabla) \oplus R(\nabla)^{\perp_{\hat{\sigma}}}$$

where

$$\begin{aligned} R(\nabla) &= \{\nabla\varphi : \varphi \in G_0\} \\ R(\nabla)^{\perp_{\hat{\sigma}}} &= \{K \in C_0 : \textstyle\int_\Omega \hat{\sigma}K\cdot\nabla\varphi = 0 \ \forall_{\varphi\in G_0}\} \end{aligned}$$

Let the solution E to equation (2) be represented by

$$E = \nabla\varphi_E + E_\perp \quad \varphi_E \in G_0,\ E_\perp \in R(\nabla)^{\perp_{\hat{\sigma}}}$$

By setting $K = K_\perp \in R(\nabla)^{\perp_{\hat{\sigma}}}$ and then $K = \nabla\varphi$, one can show that (2) is equivallent to two uncoupled equations on $R(\nabla)^{\perp_{\hat{\sigma}}}$ and $R(\nabla)$ respectively.

$$\begin{aligned} \textstyle\int_\Omega \frac{1}{\mu}\nabla\times E_\perp\cdot\nabla\times K_\perp + i\omega\int_\Omega \hat{\sigma}E_\perp\cdot K_\perp &= \textstyle\int_\Omega J^{imp}\cdot K_\perp \\ i\omega\textstyle\int_\Omega \hat{\sigma}\nabla\varphi_E\cdot\nabla\varphi &= \textstyle\int_\Omega J^{imp}\cdot\nabla\varphi \end{aligned}$$

Imposing the second of the two equations is called divergence correction. This correction is important when $\omega\hat{\sigma}$ is small.

Edge elements on hexahedral grid are designed in such a way that the Hodge decomposition holds, if one considers the gradient operating on the space of node shape functions defined on the same grid (Bochev & Gunzburger, 2006). Divergence correction requires solving a Poisson equation which has 3 times less variables, and the matrix has three times smaller bandwidth, than the finite element system matrix. Thus to store the correction matrix in a banded dense format one needs 9 times less memory, and the factorization is about 10 times faster, than for the system matrix.

NUMERICAL RESULTS

Models considered

First we consider two models of a prism in a half space. The prism has dimensions 2km x 1km x 2km and its upper side is buried 500m below the ground. The conceptual plot of this model is presented on Figure 1. Both coarser and finer discretization grids are computed, with the central portion of the finer presented in Figure 2.

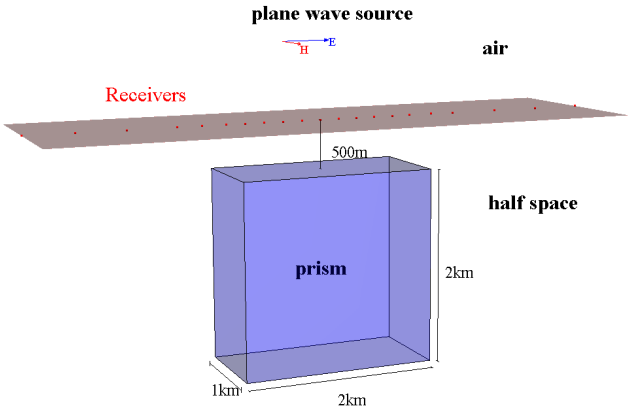

Figure 1. Conceptual plot of a prism in half space model

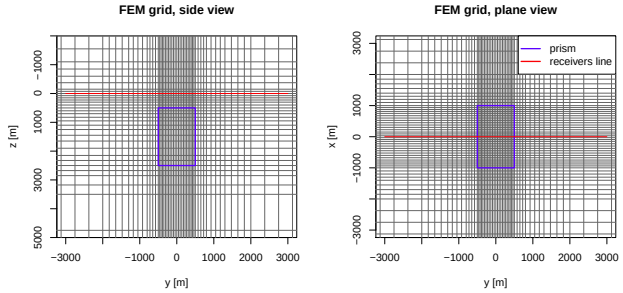

Figure 2. Central portion of the hexahedral grid for finer mesh for prisms in half-space; side and plane view

The first model is a conductive (1Ωm) in a 100Ωm half-space. The second model is a resistive (1000Ωm) prism in a 10Ωm half-space. For both of the prism models we calculate the electric field with plane wave source going downwards, with incident electric field in x-direction and magnetic field in y-direction. The code solves for the scattered field — the difference between the total E-field with the prism and the E-field of half space background only.

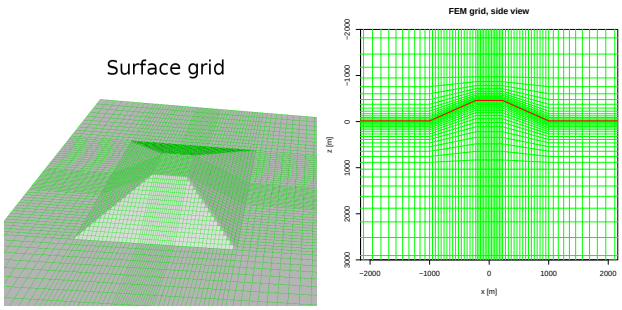

Figure 3. Central portion of the finer grid for 3-D hill model

The third model is the 3D trapezoidal hill considered in (Nam et al., 2007). The hill is 0.45 km high, 0.45 km wide at the hilltop and 2 km wide at the base. The calculations are

done for a single frequency 2Hz, and the magnetotelluric response is compared with the response in (Nam et al., 2007). The finer grid of two grids considered is presented in Figure 3.

Calculated field

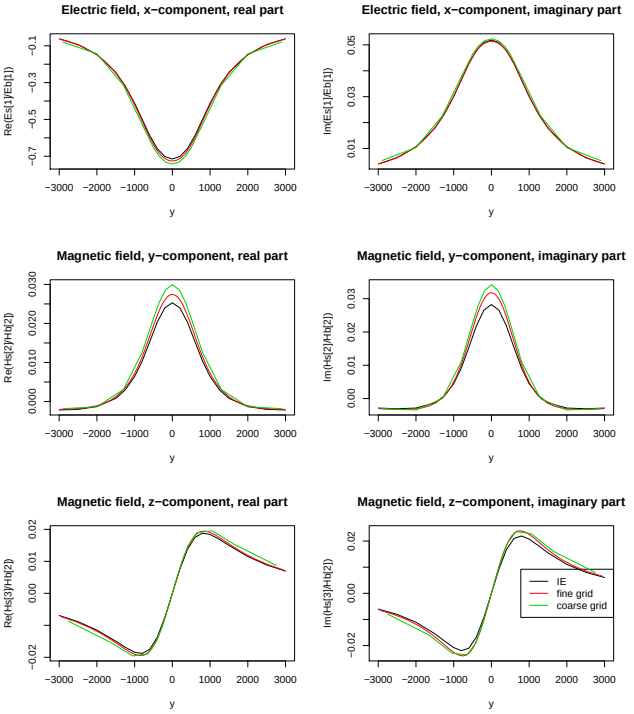

Figure 4. The electric field E and magnetic field H calculated for a **conductive prism** (1Ωm) in a 100Ωm half-space; frequency $\mathbf{0.1Hz}$

For the coarse prism grid of 21x22x23 elements, there were 29,042 unknowns, while for the finer grid of 85x88x46 elements there were 1,001,583 unknowns. The factorization of the system matrix, using 24-core CPU took 10 seconds, and 2 hours and 15 minutes, for the coarse and fine prisms respectively. Electric and magnetic fields at the surface calculated for the conductive prism, normalized by their primary fields, are compared with those from the Integral Equation (IE) code (Wannamaker., 1991) in Figure 4 at 0.1 Hz. For the IE computations, the prism was divided into 20 bricks of equal dimension in the x-y-z directions. Agreement appears good for both discretizations. Similarly good agreement was obtained for 10Hz and 0.001Hz, but is not plotted to save space. For the model of a resistive prism in a half space, the agreement between methods is good as well at 0.1Hz (figure 5), and similarly for 10Hz and 0.001Hz.

For the 3D-hill model two grids were tried. The finer grid has 97x97x50 elements and as a result the number of unknowns (edges inside the domain) is 1,373,376. To store the system matrix in dense banded format, 301GB was needed. The factorization of the system matrix, using 24 core-CPU took 4 hours and 46 minutes. A coarser grid has 27x27x24 elements, the number of unknowns is 48,516, the memory needed to store the system matrix is 1.4GB, and the factorization time is 30 s.

Our values for apparent resistivity and phase from the MT impedance elements Z_{xy} and Z_{yz} are compared in Figure 6 with those in Nam et al (2007), which we have digitized. The agreement between the results is considered very good. Apart from using a direct solver, it is worth noting that both our and the Nam formulations are the same: edge finite elements of the first order on hexahedral grid. The grids presented here also differ from Nam et al, which was 31x31x24. In part the large grid was computed to test direct solution run times for model sizes that could be practical for moderately large field data sets.

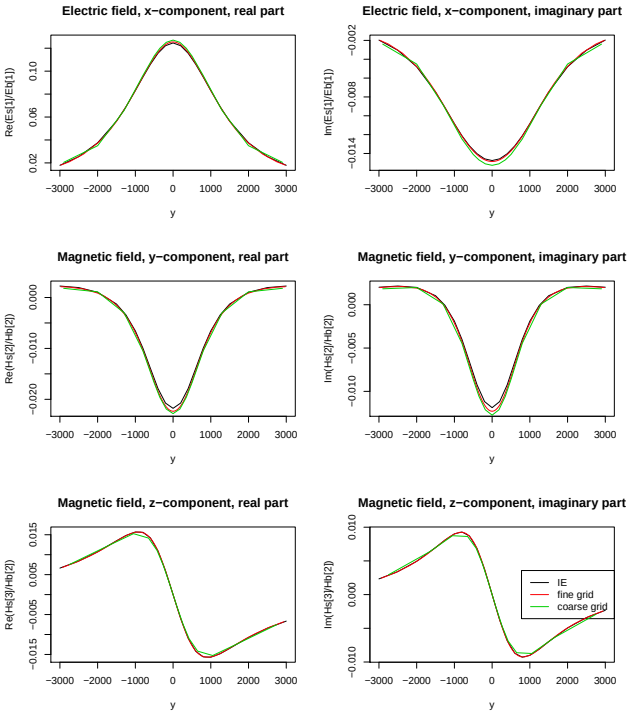

Figure 5. The electric field E and magnetic field H calculated for a **resistive prism** (1000Ωm) in a 10Ωm half-space; frequency $\mathbf{0.1Hz}$

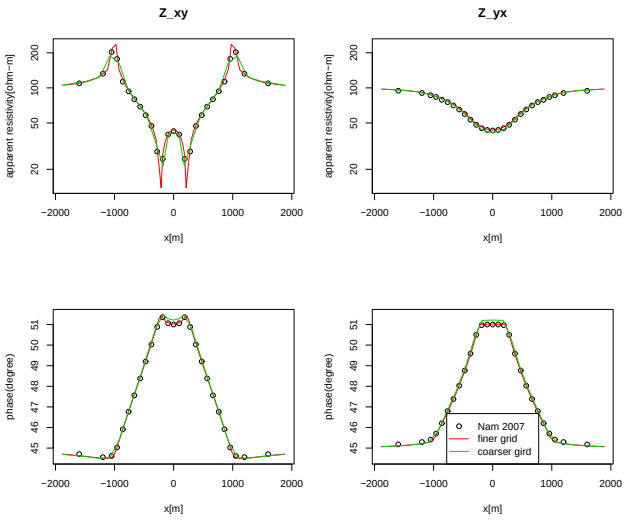

Figure 6. The apparent resistivity and the phase calculated for Z_{xy} and for Z_{yx} for a 3-D hill model

Divergence correction

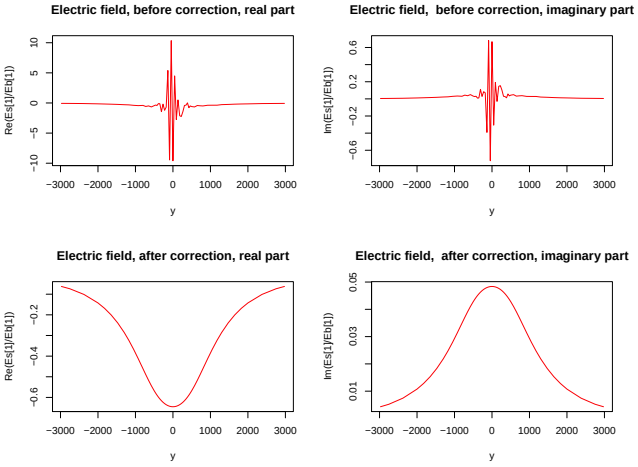

Figure 7. The electric field E calculated for a conductive prism (1Ωm) in a 100Ωm half-space; calculated **in the air**, at height 75m; frequency **0.1Hz**; before and after divergence correction

Using our conductive prism as an example, the electric field response at 0.1Hz before and after the divergence correction is presented in Figure 7. One can observe that the field values before the correction have large numerical error especially over center of the body which divergence correction successfully removes. The divergence error is even worse at the lower frequency of 0.001Hz, but again can be fully corrected as in Figure 8. It is worth noting that the magnetic field in the air (not plotted), which is calculated using curl of the electric field (see equation (7)) is not affected by the parasitic solution and has the same (proper) value before and after the correction. The divergence problem was not visible at the frequency 10Hz.

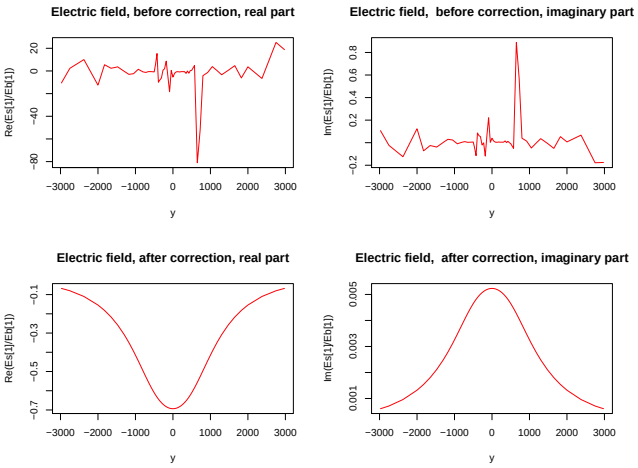

Figure 8. The electric field E calculated for a conductive prism (1Ωm) in a 100Ωm half-space; calculated **in the air**, at height 75m; frequency **0.001Hz**; before and after divergence correction

Direct solver scalability

A parallel factorization algorithm, that uses a matrix tiling approach in modified Cholesky (LDLT) factorization, described in detail in Maris and Wannamaker (2010), has been adapted to complex valued and banded matrices. The scalability of the direct solver, measured in the speedup in the factorization time depending on the number of cores used, is presented in Figure 9. The values were calculated on a model with grid: 53x53x38, number of unknowns: 306,696, and the system matrix in the dense banded format needed 28GB. We achieve nearly linear speedup versus number of cores. Efficiency of this process is still being researched, for example determining the optimal tile size relative to processor cache memory.

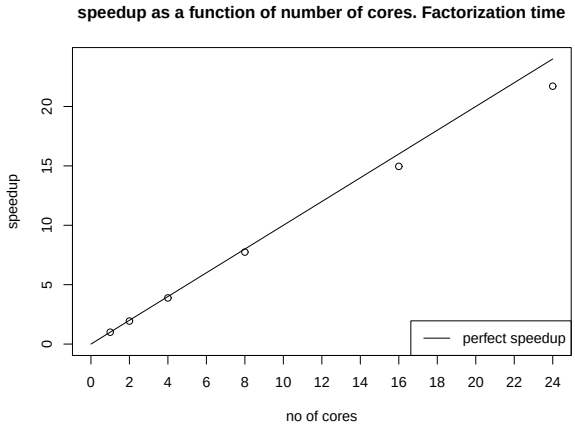

Figure 9. Scalability of the factorization measured in speedup (time of factorization using one core/ time of factorization using n cores)

ACKNOWLEDGEMENTS

This research and presentation was supported under U.S. Dept. of Energy contract DE-EE0002750 to P. Wannamaker.

REFERENCES

Bochev, P., & Gunzburger, M. (2006). Least-squares finite element methods. In *Proceedings of the international congress of mathematicians (icm)*. Madrid.

Maris, V., & Wannamaker, P. E. (2010, October). Parallelizing a 3D finite difference MT inversion algorithm on a multicore PC using OpenMP. *Computers and Geosciences*, *36*, 1384-1387.

Nam, M. J., Kim, H. J., Song, Y., Lee, T. J., Son, J. S., & Suh, J. H. (2007). 3D magnetotelluric modelling including surface topography. *Geophysical Prospecting*, *55*, 277-287.

Smith, J. (1996). Conservative modeling of 3-d electromagnetic fields, part ii: Biconjugate gradient solution and an accelerator. *Geophysics*, *61*(5), 1319-1324.

Wannamaker., P. (1991). Advances in three-dimensional magnetotelluric modeling using integral equations. *Geophysics*, *56*, 1716-1728.